Diffusion MRI reconstruction contest/workshop

May 02, 2012

Centre Convencions International Barcelona (CCIB)
Barcelona, Spain
room 124

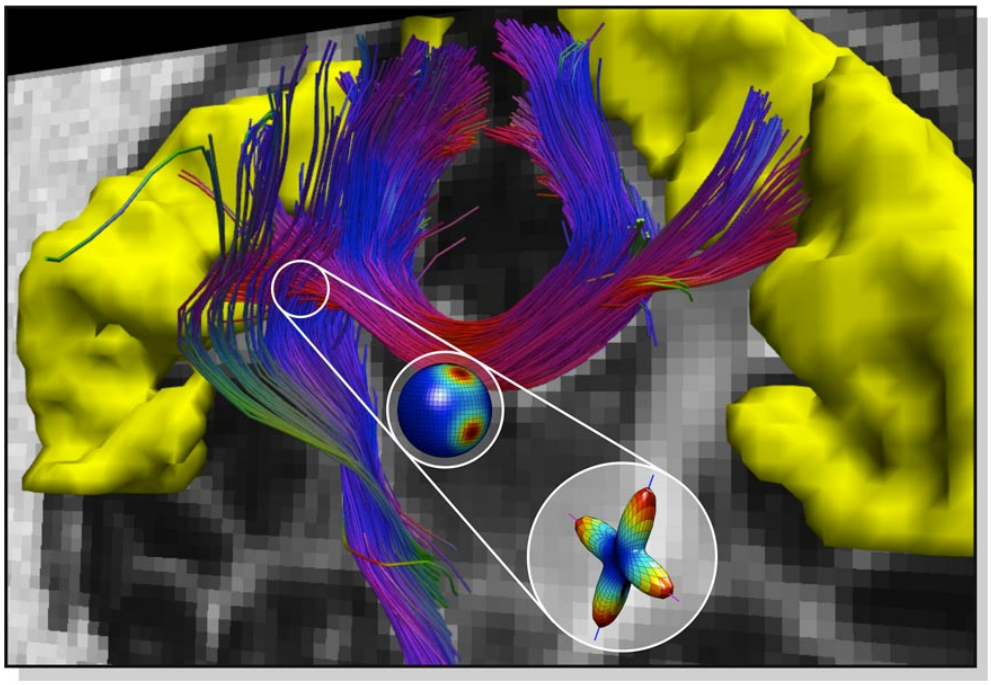

Background

The anisotropy of diffusion in white matter can be exploited for mapping the structural neuronal connectivity of the brain, and structures invisible with other imaging modalities can be highlighted. The study of this connectivity is of course of major importance in a fundamental neuroscience perspective, for developing our understanding of the brain, but also in a clinical perspective, with particular applications for the understanding of diseases like stroke or schizophrenia. As a consequence, our ability to achieve high angular resolution diffusion magnetic resonance imaging (MRI) represents an important challenge for neuroscience.

The state-of-the-art Diffusion Spectrum Imaging (DSI) modality, which relies on Cartesian signal sampling, is known to provide good imaging quality but is significantly too time-consuming to be of real interest in a clinical perspective. Accelerated acquisitions, relying on a smaller number of sampling points, are thus required. In the last few years, an increasing number of techniques have been proposed to recover the fiber directions inside the brain from diffusion MRI data. Some of them aim at reducing the long acquisition times required in diffusion MRI, while others focus on increasing the sensitivity and the angular resolution of the reconstructions.

Motivation

The present **diffusion MRI reconstruction contest/workshop** was organized with the aim to provide a way for different groups to propose their own algorithms and to fairly compare their methods against the others on a common set of ground-truth data.

The **goal** of this event is to gather researchers working in this field around a table to *discuss*, *share thoughts* and *explore new challenges* in the exciting field of diffusion MRI signal modelling and reconstruction.

Organizing committee

Alessandro Daducci	École Polytechnique Fédérale de Lausanne (EPFL), Switzerland
Yves Wiaux	École Polytechnique Fédérale de Lausanne (EPFL), Switzerland University of Geneva, Switzerland
Jean-Philippe Thiran	École Polytechnique Fédérale de Lausanne (EPFL), Switzerland University of Lausanne, Switzerland

Agenda

08.30 - 08.40 Welcome and opening

08.40 - 08.52 **Evaluation of the Deconvolved Diffusion Spectrum Imaging Technique**
Erick Jorge Canales-Rodríguez

08.52 - 09.04 **Cartesian grid q-space reconstruction**
Eleftherios Garyfallidis

09.04 - 09.16 **Propagator denoising in sparse domains: is SWT a viable solution?**
Ying-Chia Lin

09.16 - 09.28 **Multi-Tensor Fitting Guided by ODF Estimation**
Erick Jorge Canales-Rodríguez

09.28 - 09.50 **Testing classical single-shell HARDI techniques**
Maxime Descoteaux

09.50 - 10.00 Buffer / Small break

10.00 - 10.12 **Fiber Orientations Assessment via Symmetric Tensor Decomposition**
Yaniv Gur

10.12 - 10.24 **Taming diffusion to the next level**
Paulo Rodrigues

10.24 - 10.36 **Parametric Dictionary Learning in Diffusion MRI**
Emmanuel Caruyer

10.36 - 10.48 **Sparse ℓ_1-ℓ_1 Multi-Tensor Imaging at the Price of DTI**
Michael Paquette

10.48 - 11.00 **Diffusion Basis Functions on Spatially Regularized DW-MRI**
Omar Ocegueda

11.00 - 11.30 Coffee break

11.30 - 11.42 **Compressed Sensing Reconstruction of Multi-Tensor Models**
Merry Mani

11.42 - 11.54 **L1-based ODF Estimation with Total Generalized Variation**
Marco Reisert

11.54 - 12.15 Results

12.15 - 12.55 Round table discussion

- Results: is there a real "winner"?
- Evaluation framework: pitfalls, improvements, comments
- What have we learned?
- Where to go from here?

12.55 - 13.00 Closing

Contest participants

Tocororo01	**Erick Jorge Canales-Rodríguez, Lester Melie-García, Yasser Iturria-Medina, Yasser Alemán-Gómez** *CIBERSAM and FIDMAG Hermanas Hospitalarias Benito Menni CASM (Barcelona, Spain), Cuban Neuroscience Center (Havana, Cuba), Department of Experimental Medicine and Surgery, Hospital General Universitario Gregorio Marañón (Madrid, Spain)*	37 samples b = 3333
Tocororo02	**Erick Jorge Canales-Rodríguez, Lester Melie-García, Yasser Iturria-Medina, Yasser Alemán-Gómez** *CIBERSAM and FIDMAG Hermanas Hospitalarias Benito Menni CASM (Barcelona, Spain), Cuban Neuroscience Center (Havana, Cuba), Department of Experimental Medicine and Surgery, Hospital General Universitario Gregorio Marañón (Madrid, Spain)*	257 samples $320 \leq b \leq 8000$
HARDY	**Farshid Sepehrband, Jayran Chupan, Quang Tieng, Viktor Vegh, Steven Yang** *Centre for Advanced Imaging, The University of Queensland (Brisbane, Australia)*	82 samples b = 1200
HOT gang	**Yaniv Gur, Fangxiang Jiao, Stella Xinghua Zhu, Chris R. Johnson** *SCI Institute, University of Utah (Salt Lake City, USA)*	64 samples b = 3000
MrSCIL	**Michael Paquette, Maxime Descoteaux** *Sherbrooke Connectivty Imaging Lab, Sherbrooke University (Sherbrooke, Quebec, Canada)*	24 samples b = 750
MrSS	**Maxime Descoteaux, Arnaud Boré** *Sherbrooke Connectivty Imaging Lab, Sherbrooke University (Sherbrooke, Quebec, Canada)*	60 samples b = 3000
NIPG	**Ying-Chia Lin, Gloria Menegaz** *University of Verona (Verona, Italy)*	256 samples $320 \leq b \leq 8000$
Athena	**Sylvain Merlet, Emmanuel Caruyer, Aurobrata Ghosh, Rachid Deriche** *Inria (Sophia-Antipolis Méditerranée, France)*	15 samples b = 2000
Frogs	**Alonso Ramírez-Manzanares, Ramón Aranda, Mariano Rivera, Omar Ocegueda** *University of Guanajuato (Guanajuato, Mexico), Research Center on Mathematics, CIMAT, A.C., (Guanajuato, Mexico)*	48 samples b = 1500
Hawks	**Merry Mani, Mathews Jacob, Jianhui Zhong** *University of Rochester (Rochester, USA), University of Iowa (Iowa City, USA)*	30 samples b = 1200
Diffusiontamers	**Paulo Rodrigues, Vesna Prčkovska** *Universitat de Barcelona (Barcelona, Spain), IDIBAPS (Barcelona, Spain)*	12 samples b = 1000
Tyranny	**Eleftherios Garyfallidis, Ian Nimmo-Smith** *University of Cambridge (Cambridge, United Kingdom)*	257 samples $314 \leq b \leq 8011$
Frunik	**Marco Reisert, Valerij Kiselev, Henrik Skibbe** *Department of Radiology, University Medical Center (Freiburg, Germany)*	64 samples $1500 \leq b \leq 2500$

Proceedings

Evaluation of the Deconvolved Diffusion Spectrum Imaging Technique

Erick Jorge Canales-Rodríguez*† Lester Melie-García‡ Yasser Iturria-Medina‡ and Yasser Alemán-Gómez†§
* FIDMAG Hermanas Hospitalarias (Barcelona, Spain)
† Centro de Investigación Biomédica en Red de Salud Mental (CIBERSAM), (Madrid, Spain)
‡ Neurophysics Department, Cuban Neuroscience Center (CNEURO) (Havana, Cuba)
§ Department of Experimental Medicine and Surgery, Hospital General Universitario Gregorio Marañón (Madrid, Spain)

DIFFUSION-MRI RECONSTRUCTION CONTEST

Results presented at the "High Angular Resolution Diffusion MRI Reconstruction Techniques" Workshop within the IEEE International Symposium on Biomedical Imaging (ISBI 2012). For more details see the contest website http://hardi.epfl.ch/contest.html.

TECHNICAL DESCRIPTION

Simulated Data

All synthetic data were generated using a standard Diffusion Spectrum Imaging (DSI) sampling scheme [1], which consisted of a keyhole Cartesian acquisition to include the set of points in *q-space* lying on a Cartesian grid within a sphere of radius 5, for a total of *N* = 257 sampling points on one hemisphere. Because of the inherent antipodal symmetry, the signal was duplicated on the other hemisphere to obtain 515 points. The maximum *b-value* was 8000 s/mm^2. Two datasets corresponding to different intravoxel fiber configurations (i.e., isolated voxels and structured field) were provided by the organizers of the contest. Each dataset was contaminated with Rician noise for different signal-to-noise ratios (i.e., *SNR* = 5, 10, 15, 20, 25, 30, 35 and 40).

Description of the Reconstruction Method

ODF reconstruction: According to our previous work [2], all deconvolved DSI reconstructions were computed as follows. (1) The standard (blurred) diffusion propagator was reconstructed at each voxel by taking the 3D Fast Fourier Transform of the diffusion signal. The signal was zero-padded before the Fourier transformation in order to obtain interpolated propagators (matrix size: 35×35×35). (2) The Point Spread Function (PSF) of the experiment was determined as in [2]. However, instead of using a truncated *Sinc* function, a *Gaussian* function with approximate profile shape was employed. (3) The exact propagator was recovered by deconvolving the standard diffusion propagator and the PSF. The deconvolution process was performed using the accelerated Lucy-Richardson deconvolution algorithm. This method conserves the constraints on frequency distributions such as normalization and non-negativeness. (4) The resulting deconvolved propagator was trilinearly interpolated to a spherical lattice. The interpolation parameters were chosen to obtain 50 radial points along each of the 724 spatial directions specified in the contest. (4) Finally, the diffusion Orientational Distribution Function (*ODF*) was computed for each spatial direction $\hat{\mathbf{r}}$ by taking the following weighted radial summation: $ODF(\hat{\mathbf{r}}) = \int P(\rho, \hat{\mathbf{r}})\rho^2 d\rho$ [1], where P denotes the obtained diffusion propagator.

This work is supported by CIBERSAM

ODF filtering: In order to denoise the results, each *ODF* was expanded in terms of real spherical harmonics using the regularization approach proposed in [3]. In this implementation the maximum spherical harmonic order and the the regularization parameter were set to L_{max} =10 and $\lambda = 0.004$, respectively. Because of the DSI reconstruction for *SNR* = 5 is inaccurate, for this particular *SNR* the spherical harmonic order was L_{max} =2, which allows the extraction of only one fiber population per voxel. The final *ODF*s were recomputed from the resulting spherical harmonic coefficients.

ODF maxima extraction: Local fiber orientations were determined in two steps: First, all local maxima were obtained by comparing the *ODF* amplitudes between each point in the grid and its nearest neighbors within and interval of 15 *degrees*. The largest three local maxima were preserved if their amplitudes were above the value 0.4×ODF$_{max}$, where ODF$_{max}$ is the amplitude of the global maximum. Second, to refine the spatial positions of the resulting maxima, all neighbors around each maximum were used to fit an ellipsoid centered at the origin. The position of the principal direction of each ellipsoid was used to specify the local fiber orientation.

REFERENCES

[1] Wedeen V.J., Hagmann P., Tseng W.Y., Reese T.G., Weisskoff, R.M, "Mapping complex tissue architecture with diffusion spectrum magnetic resonance imaging", Magn Reson. Med., 54, 1377-1386 (2005).
[2] Canales-Rodríguez E.J., Iturria-Medina Y., Alemán-Gómez Y., Melie-García L., "Deconvolution in diffusion spectrum imaging", Neuroimage, 50(1), 136-149 (2010).
[3] Descoteaux M., Angelino E., Fitzgibbons S., Deriche R., "Regularized, Fast and Robust Analytical Q-Ball Imaging", Magn Reson. Med., 58(3), 497-510 (2007).

Cartesian grid q-space reconstruction

Eleftherios Garyfallidis* and Ian Nimmo-Smith†
* University of Cambridge
† MRC Cognition and Brain Sciences Unit

For the purpose of the HARDI reconstruction workshop we used GQI2 [1], [2] a non-parametric method to find the ODFs [3], [4] for dMRI acquisitions on a keyhole cartesian grid in q-space [3]. From these ODFs we find the number of peaks (number of fiber compartments); if this number equals 1, we report the ODF from fitting the Single Tensor to the data, otherwise we report the original GQI2 ODF.

Following the approach of Wedeen et al. [5] the ODF can be derived by obtaining the diffusion propagator from the dMRI signal by a Fourier transform on the cartesian lattice $P(\mathbf{r}) = \mathcal{F}(S_0^{-1}S(\mathbf{q}))$ and then integrating radially.

$$\psi_{DSI}(\hat{\mathbf{u}}) = \int_0^\infty P(r\hat{\mathbf{u}})r^2 dr \tag{1}$$

Yeh et al. [1] proposed a direct way to calculate a slightly different ODF using the Cosine transform. They estimated the spin density weighted propagator Q via from an unweighted truncated radial projection

$$\begin{aligned}\psi_{GQI}(\hat{\mathbf{u}}) &= \int_0^\lambda Q(r\hat{\mathbf{u}})dr \\ &= \lambda \int S(\mathbf{q})\mathtt{sinc}(2\pi r\mathbf{q}\cdot\hat{\mathbf{u}})d\mathbf{q}\end{aligned} \tag{2}$$

where λ is a smoothing factor called the diffusion sampling length.

We have instead developed an ODF like the one produced using DSI where we need to take into consideration the weighted truncated radial projection r^2. This will give us a different ODF which we symbolize with ψ_{GQI2}

$$\begin{aligned}\psi_{GQI2}(\hat{\mathbf{u}}) &= \int_0^\lambda Q(r\hat{\mathbf{u}})r^2 dr \\ &= \lambda^3 \int S(\mathbf{q})H(2\pi r\mathbf{q}\cdot\hat{\mathbf{u}})d\mathbf{q}\end{aligned} \tag{3}$$

where $H(x) = \begin{cases} \frac{2\cos(x)}{x^2} + \frac{(x^2-2)\sin(x)}{x^3}, & x \neq 0 \\ 1/3, & x = 0 \end{cases}$.

This equation can be implemented analytically in a simple matrix form

$$\boldsymbol{\psi}_{GQI2} = \mathbf{s}\cdot\mathtt{H}((6D.G\circ\mathbf{b}\circ\mathbb{1})\cdot G)\lambda^3/\pi \tag{4}$$

where $\cdot$ denotes standard matrix or vector dot product, $\circ$ denotes the Hadamard product, $\boldsymbol{\psi}_{GQI}$ as a MD vector with components corresponding to the selected directions $\hat{\mathbf{u}}$ on the ODF sphere, $\mathbf{s}$ is a vector with all the signal values, $D = 0.0025$ where D is the free water diffusion coefficient, G is the $N \times 3$ matrix with the gradient vectors, $\mathbf{b}$ is the $N \times 1$ matrix with the b-values and $\mathbb{1}$ is the $N \times 3$ incidence matrix where all values are equal to 1.

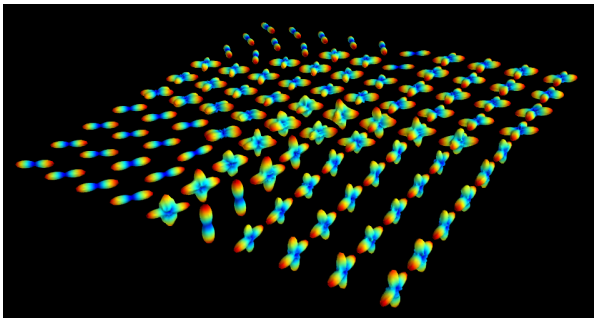

Figure 1. Result showing our reconstruction ODFs with the training data set (SNR 30) provided by the organizers of the HARDI Workshop 2012

We use $\lambda = 3.0, 3.3, 3.5$ with the provided phantom data with SNRs $10, 20, 30$ respectively. In the case where a single peak is found the Single Tensor model is fitted using Weighted Least Squares and the standard ODF for that is generated.

The source code for the methods described here can be found in DIPY (dipy.org). An example of our method can be seen in Fig. 1. GQI2 is a method theoretically identical with the framework of Equatorial Inversion Transform (EIT) [2] with Laplacian weighting. This builds on the formulation in eq. 4.

Model-based methods for ODF estimation, like the Single Tensor or Multi Tensor, require a number of parameters to be fitted. By contrast for model-free methods fitting is not necessary and the directionality of the underlying tissue can be approximated by a re-parametrization or re-transformation of the signal. The latter is usually more efficient than fitting models with many parameters which typically call for iterative methods.

References

[1] F. Yeh, V. Wedeen, and W. Tseng, "Generalized Q-sampling imaging," *IEEE Transactions on Medical Imaging*, vol. 29, pp. 1626–1635, Mar. 2010.

[2] E. Garyfallidis, *Towards an accurate brain tractography*. PhD thesis, University of Cambridge, 2012.

[3] D. S. Tuch, T. G. Reese, M. R. Wiegell, N. Makris, J. W. Belliveau, and V. J. Wedeen, "High angular resolution diffusion imaging reveals intravoxel white matter fiber heterogeneity," *Magnetic Resonance in Medicine*, vol. 48, no. 4, pp. 577–582, 2002.

[4] I. Aganj, C. Lenglet, G. Sapiro, E. Yacoub, K. Ugurbil, and N. Harel, "Reconstruction of the orientation distribution function in single- and multiple-shell q-ball imaging within constant solid angle," *Magnetic Resonance in Medicine*, vol. 64, no. 2, pp. 554–566, 2010.

[5] V. J. Wedeen, R. P. Wang, J. D. Schmahmann, T. Benner, W. Y. Tseng, G. Dai, D. N. Pandya, P. Hagmann, H. D'Arceuil, and A. J. de Crespigny, "Diffusion spectrum magnetic resonance imaging (DSI) tractography of crossing fibers.," *Neuroimage*, vol. 41, no. 4, pp. 1267–77, 2008.

Propagator denoising in sparse domains: is SWT a viable solution?

Ying-Chia Lin*, Gloria Menegaz*
* Department of Computer Science, University of Verona, Italy

***Abstract*—The proposed approach consists in wavelet-based denoising of Diffusion Spectrum Imaging (DSI) data. The data were first reconstructed by inverse Fourier transform and then projected to the multiscale domain by 3D Stationary Wavelet Transform (3D-SWT). Then, denoising was performed by soft and hard thresholding such that a fixed percentage of coefficient was retained. Different families of wavelets and decomposition depths were considered and performance was evaluated according to the Kullbach-Leibler divergence among the reference and the denoised Orientation Distribution Functions (ODFs). Results revealed that the D4 family with a single level of decomposition provides the best solution.**

A. Methods

The sparsity theory states that it is possible to recover signals and images from far fewer samples or measurements than those that traditional methods suggest[1]. In this work, we propose to use the three dimensional Stationary Wavelet Transform (3D-SWT) for sparsifying the data followed by thresholding for denoising in wavelet domain. First steps in this direction were taken in [5] where different families of discrete wavelet transforms (DWT) were considered. Though, DWT suffers from the lack of shift invariance. In order to overcome this limitation and improve the performance we rely on SWT [3], [6], [2]. Accordingly, the data were first projected in the signal domain by inverse 3D Fourier transform, and then sparsified by projection to the 3D-SWT domain where thresholding was performed. The D4, D8 and CDF5/3 wavelet families were considered. Hard and soft thresholding were performed by applying via the respective operators (ρ_H and ρ_S) to the wavelet coefficients [4]

$$\rho_H(x) = \begin{cases} x & \text{if} \quad x \geq T \\ 0 & \text{if} \quad x < T \end{cases} \tag{1}$$

$$\rho_S(x) = \begin{cases} x - T & \text{if} \quad x \geq T \\ x + T & \text{if} \quad x \leq -T \\ 0 & \text{if} \quad x < |T| \end{cases} \tag{2}$$

The value of the threshold T was set to the 5%, respectively 10% of the noise standard deviation. Additionally, Donoho and Johnstone universal threshold was used.

The dataset was obtained by simulations and four different levels of noise were considered corresponding to $SNR = 10, 20, 30, 40$. For each noise level, 100 realizations of the noisy signal were generated and processed. Two different decomposition depths were considered, namely $L = 1, 2$, respectively. Performance was assessed by the Kullback-Leibler Divergence (KLD) between the ground truth ODF (f) and the denoised one ($\tilde{f}$) according to

$$D_{KLD}(\tilde{f}, f) = \sum_x \tilde{f}(x) \cdot log_2 \left\{ \frac{\tilde{f}(x)}{f(x)} \right\}. \tag{3}$$

Results are illustrated in Fig.1, where the box plots highlight the mean and standard deviation of the KLD measurements over the set of realizations for all the considered settings for $SNR = 10$. Similar plots were obtained for the other noise levels. Best performance was obtained with D4 and $L = 1$. In the figure, the noisy signal is labelled as DSI. The identification of the best T/σ ratio is currently under investigation.

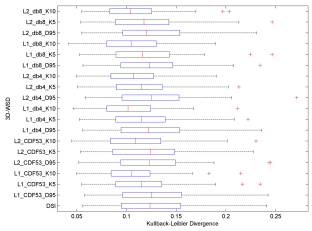

Fig. 1. KLD between the reference and denoised ODFs at changing experimental conditions for $SNR = 10$.

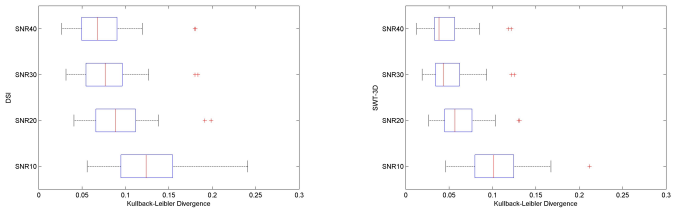

(a) (b)

Fig. 2. KLD between the reference and (a) noisy (b) denoised ODFs for the best solution at changing SNRs.

Fig.2 (a) and (b) represent the box plots of the KLD over the different realizations between pairs of noise-free (noisy) ODF and the respective denoised versions for all the considered noise levels and for the best configuration ($L = 1$, D4). As it can be observed, the KLD is reduced by SWT denoising in all conditions. An extended set of experimental conditions (T/σ ratio, number of decomposition levels) will allow the optimization of the denoising framework.

References

[1] E. J Candes and M. B Wakin. An introduction to compressive sampling. *IEEE Signal Processing Magazine*, 25(2):21–30, March 2008.

[2] P. Celka, K.N. Le, and T.R.H. Cutmore. Noise reduction in rhythmic and multitrial biosignals with applications to Event-Related potentials. *Biomedical Engineering, IEEE Transactions on*, 55(7):1809 –1821, July 2008.

[3] M. Lang, H. Guo, J.E. Odegard, C.S. Burrus, and Jr. Wells, R.O. Noise reduction using an undecimated discrete wavelet transform. *Signal Processing Letters, IEEE*, 3(1):10 –12, January 1996.

[4] Stephane Mallat. *A Wavelet Tour of Signal Processing, 3rd ed., Third Edition: The Sparse Way*. Academic Press, December 2008.

[5] E. Saint-Amant and M. Descoteaux. Sparsity characterisation of the diffusion propagator. *International Society for Magnetic Resonance in Medicine (ISMRM' 11)*, 2011.

[6] X.H. Wang, R.S.H. Istepanian, and Yong Hua Song. Microarray image enhancement by denoising using stationary wavelet transform. *NanoBioscience, IEEE Transactions on*, 2(4):184 –189, December 2003.

Multi-Tensor Fitting Guided by ODF Estimation

Erick Jorge Canales-Rodríguez*† Lester Melie-García‡ Yasser Iturria-Medina‡ and Yasser Alemán-Gómez†§
* FIDMAG Hermanas Hospitalarias (Barcelona, Spain)
† Centro de Investigación Biomédica en Red de Salud Mental (CIBERSAM), (Madrid, Spain)
‡ Neurophysics Department, Cuban Neuroscience Center (CNEURO) (Havana, Cuba)
§ Department of Experimental Medicine and Surgery, Hospital General Universitario Gregorio Marañón (Madrid, Spain)

DIFFUSION-MRI RECONSTRUCTION CONTEST

Results presented at the "High Angular Resolution Diffusion MRI Reconstruction Techniques" Workshop within the IEEE International Symposium on Biomedical Imaging (ISBI 2012). For more details see the contest website http://hardi.epfl.ch/contest.html.

TECHNICAL DESCRIPTION

Simulated Data

The diffusion signal was simulated following the *multi-tensor* model, using $N = 37$ sampling points on one hemisphere and a constant *b-value* equal to 3333 s/mm^2. The sampling points were obtained by means of the approach proposed in [1], which introduces a method for locating *N* equal nonoverlapping circles on a hemisphere. Two datasets corresponding to different intravoxel fiber configurations (i.e., isolated voxels and structured field) were provided by the organizers of the contest. Each dataset was contaminated with Rician noise for different signal-to-noise ratios (i.e., *SNR* = 5, 10, 15, 20, 25, 30, 35 and 40).

Description of the Reconstruction Method

Reconstructions based on the *multi-tensor* model are unstable and lose accuracy when the number of tensors used in the model differs from the number of fiber populations in the voxel. One alternative to *multi-tensor* fitting is the Orientational Distribution Function (*ODF*) estimation based on *q-space* methods. The *ODF* along nerve fibers is much higher than across fibers. Consequently, the number of fiber-compartments, their relative amplitudes and spatial orientations can be inferred from the *ODF* local maxima. However, methods using *ODF* reconstructions have to deal with two major limitations. One, these methods are not able to quantify the anisotropy contribution of each individual fiber compartment. Two, the obtained *ODF*s are over-smoothed representations of the true *ODF*s because they are computed using low-frequency basis functions. In order to alleviate these two problems, the following processing steps are proposed: (1) *ODF* reconstruction, (2) *ODF* filtering and sharpening, (3) *ODF* maxima extraction and (4) Multi-tensor *ODF* fitting. Each step will now be explained.

(1) ODF Reconstruction: The *ODF* reconstruction method implemented in this work is described in [2]. The particular solution employed here corresponds to the *second-order* radial projection *ODF*, which includes the Jacobian for spherical coordinates. The *ODF*s were computed using real spherical harmonics and the regularized inversion approach proposed in [3]. The optimal regularization parameter λ was calculated for each voxel by means of the Cross-Validation technique. Terms up to $L_{max} = 4$ were included in all calculations.

This work is supported by CIBERSAM

(2) ODF Filtering and Sharpening: To increase the spatial coherence of the *ODF*-fields in the structured field dataset, a spatial anisotropic smoothing was applied to each volume-image created from the spherical harmonic coefficients at each particular order. A network structure of 26 neighbouring voxels was considered for diffusion conduction. From the different available methods in the literature, the exponential function proposed in [4] was selected because it maintains high-contrast edges over low-contrast ones (i.e., the smoothing process along different adjacent tracts is severely penalized).

A sharp *ODF* was obtained from the resulting *ODF* using basis functions in a dictionary-based approach. The basis functions were created by expanding delta functions (oriented along each of the 724 spatial directions specified in the contest) in terms of real spherical harmonics via the same inversion approach used to compute the *ODF*. These functions represent the Point Spread Function (PSF) of our reconstruction method. Finally, the sharp *ODF* was recovered via linear inversion (deconvolution) using Tikhonov regularization.

(3) ODF Maxima Extraction: Local fiber orientations were determined from the sharp *ODF* in two steps: (i) All local maxima were obtained by comparing the *ODF* amplitudes between each point in the grid and its nearest neighbors within and interval of 15 *degrees*. The largest three local maxima were preserved if their amplitudes were larger than $0.4\times\text{ODF}_{max}$, where ODF_{max} is the amplitude of the global maximum. (ii) To refine the spatial positions of the resulting maxima, all neighbors around each maximum were used to fit an ellipsoid centered at the origin. The position of the principal direction of each ellipsoid was used to specify the local fiber orientation.

(4) Multi-Tensor ODF Fitting: A non-linear fitting procedure was implemented to obtain the true diffusivites corresponding to each different fiber population in the voxel. The algorithm computes the diffusivities that minimizes the least-squares difference between the theoretical *ODF*, corresponding to a *multi-tensor* model, and the measured *ODF*. The number of fiber populations, their relative intensities and spatial orientations were assumed to be known and equal to the values determined in previous sections. The final *ODF* was recomputed from the *multi-tensor* fitted model.

REFERENCES

[1] Appelbaum J., Weiss Y., "The packing of circles on a hemisphere", Meas. Sci. Technol., 10, 10151019 (1999).
[2] Canales-Rodríguez E.J., Lin C.P., Iturria-Medina Y., Yeh C.H., Cho K.H., Melie-García L., "Diffusion orientation transform revisited", Neuroimage, 49(2), 1326-1339 (2010).
[3] Descoteaux M., Angelino E., Fitzgibbons S., Deriche R., "Regularized, Fast and Robust Analytical Q-Ball Imaging", Magn Reson. Med., 58(3), 497-510 (2007).
[4] Perona P. and Malik J., "Scale-Space and Edge Detection Using Anisotropic Diffusion", IEEE Trans. Pattern Anal. Mach. Intell., 12(7), 629-639 (1990).

Testing classical single-shell HARDI techniques

Maxime Descoteaux*, Arnaud Boré*
* Sherbrooke Connectivity Imaging Lab (SCIL), Computer Science department, Université de Sherbrooke

I. Introduction

The goal of this submission is to provide a set comparitive results using some of the most common HARDI reconstruction techniques having made their mark in the local reconstruction community in the last several years. Namely, we have ran analytical q-ball (a-QBI) and normalized analytical q-ball, also called constant solid angle (CSA-QBI), with different spherical harmonics (SH) orders. We have also ran spherical wavelet tranformation (SWT) of the orientation distribution function (ODF). Finally, we have ran spherical deconvolution (SD) with contrained regularization at different SH orders using two implementations. The first, from the q-ball ODF to obtain the fiber ODF (fODF) and, second, from the raw signal to obtain the fiber orientation distribution (FOD).

II. Single-shell HARDI techniques tested

A. Analytical q-ball imaging (a-QBI)

We used our in-house implementation of [1] with regularization parameter $\lambda = 0.006$ and SH order $L = 4, 6$ and 8. Recall that this QBI solution is actually a smoothed approximation of the ODF, Ψ, since it is derived from the ODF definition without the Jacobian term in the ODF integral, i.e. $\Psi(\theta, \phi) = \int_0^\infty P(r, \theta, \phi)dr$, where P is the diffusion propagator describing the 3D diffusion of water molecules.

B. Constant solid angle q-ball imaging (CSA-QBI)

We used our in-house implementation of the analytical technique presented in [2], [3] using spherical harmonics order $L = 4, 6$ and 8. Recall that this technique finds a solution to the previous equation with the proper r^2 term in the integral, i.e. $\Psi(\theta, \phi) = \int_0^\infty P(r, \theta, \phi)r^2dr$. A regularization parameter $\lambda = 0.006$ was also used.

C. ODF sharpening with spherical wavelets

We also tested the technique of [7] for SH order $L = 8$. Recall that this is a sharpening transform of the ODF. It decomposes the a-QBI ODF into low and high frequency components using a multi-resolution *à trou* spherical wavelet decomposition. Only the high-frequency ODF part, or sharpened ODF, is used to detect maxima.

D. Spherical deconvolution

Finally, we tested two SD techniques: the one presented in [4] and and the other in [5]. For both techniques, a constrained regularization implementation is used, at orders $L = 6, 8, 10$, and diffusion profile of [17, 3, 3] x10^{-6}mm^2/s is used as single-fiber deconvolution model. We found it the best trade-off and choice from the training data. The techinique [4] is implemented in our in-house tools, whereas the one of [5] uses *mrtrix* [6].

III. Solution for the ISBI contest

To respect clinical-like acquisition time and real data acquisition settings from the literature, we have limited our number of diffusion measurements to 60 directions. On the training data, we have first used the number of peaks detected as our quantitative quality measure of reconstruction. Then, we have varied the number of directions for $N = 30, 35, 40, 45, 50, 55, 60$ diffusion directions, SNR $= 5, 10, 15, 20, 25, 30, 35, 40$ and b-values $= 700, 1000, 1500, 2000, 2500, 3000, 3500$ s/mm^2. Peaks are extracted using finite differences on the ODF 724 mesh points and volume fractions of fiber crossings using a normalized ratio of the ODF peaks. The sum of ratios must equal 1.

Based on these simulations, the optimal configuration, on average, over the different phantoms, SNRs, number of measurements and b-values was $N = 60$ and $b = 3000$s/mm^2. However, none of the techniques outperformed all the others when considering all SNRs and all phantoms. This is not surprising. On the independent voxels (IV), the fODF of order $L = 6$ was the best with success of detecting all peaks at approximately 52%. On the other hand, a success rate of 80% was obtained on the structured field (SF) in 3D; from the FOD of *mrtrix* for SNRs between 10 and 25, and from the CSA-QBI/fODF/FOD/SWT for higher SNRs (almost all equal in terms of success rate). Note that for SNR 5, a-QBI of order 4, which is the technique to the most intrinsic smoothing, was best with approximately 50% sucess rate. Hence, a hybrid technique would have probably best for the datasets presented in this ISBI contest.

IV. Conclusion

Overall, when averaging over both phantoms and all SNRs, CSA-QBI of order 4, fODF of order 6 and FOD of order 8 from *mrtrix* was best at correctly finding peaks. The problem with these SD techniques is that they do not provide a diffusion ODF but a sharp angular profile. We could have generated a synthetic diffusion ODF from the peaks fODF or FOD but, instead, we decided to go with CSA-QBI of order that reconstructs a diffusion ODF close to the ground truth. Therefore, our selected "*best*" technique for the competition is **constant solid angle q-ball imaging with spherical harminics order 4**. Nonetheles, we have submitted all reconstructions described in this abstract to the organizers to include them in the global comparisons of techniques.

References

[1] Descoteaux, M., Angelino, E., Fitzgibbons, S., and Deriche, R. "Regularized, fast, and robust analytical Q-ball imaging". Magnetic Resonance in Medicine, 58(3), 497-510, 2007.

[2] Aganj, I., Lenglet, C., Sapiro, G., Yacoub, E., Ugurbil, K., and Harel, N. "Reconstruction of the orientation distribution function in single- and multiple-shell q-ball imaging within constant solid angle". Magnetic Resonance in Medicine, 64(2), 554–566, 2010.

[3] Tristan-Vega, A., Westin, C.-F., and Aja-Fernandez, S. "A new methodology for the estimation of fiber populations in the white matter of the brain with the Funk-Radon transform". NeuroImage, 49(2), 1301-1315, 2010.

[4] Descoteaux, M., Deriche, R., Knoesche, T. R., and Anwander, A. "Deterministic and probabilistic tractography based on complex fibre orientation distributions". IEEE transactions on medical imaging, 28(2), 269-86, 2009.

[5] Tournier, J.-D., Calamante, F., and Connelly, A. "Robust determination of the fibre orientation distribution in diffusion MRI: Non-negativity constrained super-resolved spherical deconvolution". NeuroImage, 35(4), 1459-1472, 2007.

[6] Tournier, J.-D., Calamante, F., and Connelly, A. "MRtrix: Diffusion tractography in crossing fiber regions". International Journal of Imaging Systems and Technology, 22(1), 53-66, 2012.

[7] Kezele, I., Descoteaux, M., Poupon, C., Poupon, F., and Mangin, J.-F. "Spherical wavelet transform for ODF sharpening". Medical Image Analysis, 14(3), 332-342, 2010.

Fiber Orientations Assessment via Symmetric Tensor Decomposition

Yaniv Gur*, Fangxiang Jiao*, Stella Xinghua Zhu† and Chris R. Johnson*
* SCI Institute, University of Utah, 72 S. Central Campus Dr., SLC, UT 84112, USA
† Department of Computer Science, The University of Hong Kong, Pokfulam Road, Hong Kong

Introduction. The majority of HARDI reconstruction techniques use an ODF to delineate the diffusion pattern within a brain voxel. The dominant diffusion directions (i.e., the fiber orientations) are extracted from the ODF using various techniques (e.g., [1]). In many cases the complexity of these techniques is high and their accuracy is limited by the quality of the ODF reconstruction. To overcome these limitations, we suggest here to reconstruct the fiber orientations and the volume fractions *directly* from the HARDI measurements, without estimating an ODF. The proposed approach relies on the spherical deconvolution technique and decomposition of homogenous polynomials by means of powers of linear-forms [2], which is known as a *symmetric tensor decomposition*. An ODF is directly related to a homogenous polynomial or a higher-order tensor [3], therefore, it could be decomposed similarly. Since an ODF encodes information on dominant diffusion directions as well as noise, to recover the dominant diffusion directions only we propose to use a lower-rank approximation of the ODF by means of power of linear-forms. In this formulation, each linear-form represent a single fiber and convolved to a single-fiber response kernel. This leads to a spherical deconvolution problem which is solved here using an iterative alternating algorithm which is based on the Levenberg-Marquardt technique.

Method. Spherical deconvolution is a common technique to recover major diffusion directions from DWI data [4]. It is based on a convolution between a spherically symmetric function, known as fODF, and an axially symmetric kernel that represents a single fiber response. Given a vector of n DWI measurements in the gradient directions, the fODF, denoted by F, is reconstructed by solving the following deconvolution problem:

$$\min_{F} \frac{1}{2} \sum_{i=1}^{n} \left\| S(\mathbf{g}_i, b) - S_0 \int_{S^2} F(\mathbf{v}) K(\mathbf{g}_i, \mathbf{v}) d\mathbf{v} \right\|^2 . \qquad (1)$$

This problem is solved for a fixed kernel, K, where its width is adjusted to the particular dataset. The resulting fODF represents a sum of spherical delta functions aligned with the fiber orientations and weighted by the volume fractions.

To combine the fODF reconstruction and the orientations estimation into one optimization problem, we first approximate the fODF using a lower-rank approximation by means of polynomial approximation (symmetric tensor decomposition) such that:

$$F(\mathbf{v}) \sim \sum_{i=1}^{\tilde{r}} \gamma_i f_i^d = \sum_{i=1}^{\tilde{r}} (\boldsymbol{\alpha}_i \cdot \mathbf{v})^d, \quad \tilde{r} < r, \qquad (2)$$

where $\boldsymbol{\alpha}_i \in \mathbb{R}^3$, $\mathbf{v} \in S^2$ and each fiber aligned in direction $\boldsymbol{\alpha}_i$ is identified with a linear form $(\boldsymbol{\alpha}_i \cdot \mathbf{v})^d$. The number of fibers to be reconstructed is determined by the approximation rank $\tilde{r}$ and the expansion coefficients are defined as $\gamma_i = \|\boldsymbol{\alpha}_i\|^d$.

Next, we substitute (2) into (1). This leads to the following non-linear optimization problem:

$$\min_{\boldsymbol{\alpha}_j} \frac{1}{2} \sum_{i=1}^{n} \left\| S(\mathbf{g}_i, b) - S_0 \int_{S^2} \sum_{j=1}^{\tilde{r}} (\boldsymbol{\alpha}_j \cdot \mathbf{v})^d K(\mathbf{g}_i, \mathbf{v}) d\mathbf{v} \right\|^2 . \qquad (3)$$

This problem is solved for the coefficients of the linear-forms(three coefficients per fiber) which are directly estimated from the DWI measurements. The fiber orientations and the volume fractions are derived as follows: Since each linear-form gets its maximum at the direction specified by $\boldsymbol{\alpha}_j$, given the optimal solution, $\tilde{\boldsymbol{\alpha}}_j$, the corresponding fiber orientation is simply $\mathbf{u}_j = \frac{\tilde{\boldsymbol{\alpha}}_j}{\|\tilde{\boldsymbol{\alpha}}_j\|}$. As we do not impose the constraint $\sum_{j=1}^{\tilde{r}} \|\boldsymbol{\alpha}_j\|^d = 1$, the corresponding volume fraction is given by $w_j = \frac{\|\tilde{\boldsymbol{\alpha}}_j\|^d}{\sum_{j=1}^{\tilde{r}} \|\tilde{\boldsymbol{\alpha}}_j\|^d}$.

The problem (3) is non-linear and we solve it here by means of the the Levenberg-Marquart (LM) optimization method. Using this method, we first reconstruct one fiber ($\tilde{r} = 1$). Then, we increment $\tilde{r} = 1$ by one and reconstruct two fibers. The solution for ($\tilde{r} = 2$) is accepted if the condition $w_2 > t_1$ holds, where w_2 is the lowest volume fraction and t_1 is a predefined threshold. If the condition holds, the rank is incremented again and three fibers are reconstructed. Otherwise, the single fiber model is selected. Similarly, the three fibers model is accepted if $w_2 > t_2$. In each case, when the rank is incremented, the solutions of the lower rank problem are used for initialization. The thresholds t_1 and t_2 were adjusted based on the training data and their values depend on the SNR. Finally, since we do not reconstruct an ODF here, we compute the ODF using the analytical solution with our estimates for the number of fibers, the volume fractions and the orientations. For each compartment we fixed the diffusivities to $[1.7, 0.4, 0.4] \cdot 10^{-3}\ mm^2 \backslash s$.

This work was funded by grants from the NSF, DOE SciDAC and NETL and the NIH NIGMS 8 P41GM103545-14.

REFERENCES

[1] I. Aganj, C. Lenglet, and G. Sapiro, "ODF maxima extraction in spherical harmonic representation via analytical search space reduction," in *MICCAI'10*, 2010, vol. 6361 of *LNCS*, pp. 84–91.

[2] Jérôme Brachat, Pierre Comon, Bernard Mourrain, and Elias P. Tsigaridas, "Symmetric tensor decomposition," *Linear Algebra and Applications*, vol. 433, no. 11-12, pp. 1851–1872, 2010.

[3] Maxime Descoteaux, Elaine Angelino, Shaun Fitzgibbons, and Rachid Deriche, "Apparent diffusion coefficients from high angular resolution diffusion imaging: Estimation and applications," *Magnetic Resonance in Medicine*, vol. 56, no. 2, pp. 395–410, 2006.

[4] J-Donald Tournier, Fernando Calamante, and Alan Connelly, "Robust determination of the fibre orientation distribution in diffusion MRI: Non-negativity constrained super-resolved spherical deconvolution," *NeuroImage*, vol. 35, no. 4, pp. 1459–1472, 2007.

Taming diffusion to the next level

Paulo Rodrigues* and Vesna Prchkovska†
* Department of Personality, Universitat Barcelona
† Institut d'Investigacions Biomdiques August Pi i Sunyer

I. Introduction

DTI has one obvious disadvantage due to the crude assumption for modelling the underlying diffusion process as Gaussian. In other words, in the areas of complex intra-voxel heterogeneity the DTI model fails to distinguish multiple fiber populations. To overcome the limitations of DTI, more complex acquisition schemes known as high angular resolution diffusion imaging (HARDI) were introduced. Even though these novel data modelling can overcome some of the drawbacks of DTI, they come with burdens of their own. In terms of clinical application, the biggest drawback of HARDI lies in the requirements for demanding acquisition schemes that result not only in datasets with high b-value and number of gradients (i.e., schemes that require long acquisition times, unattractive for clinical use) but also data heavily polluted by noise.

Our algorithm is inspired by the notion of context, and applied to diffusion weighted images (DWIs). By looking at the neighbourhood information we can "kill two rabbits at the same time", not only smooth the dataset thus removing noise, but also extrapolate information that is not there locally per-se. In this way, we are able to produce results comparable by many HARDI techniques that operate on much more demanding acquisitions, and perform better than DTI and HARDI applied on the same modest acquisition.

II. Methods

A. Acquisition scheme and diffusion tensor estimation

We used a common DTI acquisition scheme, 12 directions and b-value=1000. We estimate 2^{nd} order symmetric, positive definite diffusion tensors (DTs), using the framework of Barmpoutis [1].

B. Contextual enhancing of spherical diffusion functions from diffusion tensors

Following Prchkovska et al. [3] and Rodrigues et al. [2], once the DT is calculated per voxel, the orientation distribution function (ODF) can be reconstructed, and sampled on the sphere

$$ODF(\mathbf{n}) = \mathbf{n}^T \mathbf{D} \mathbf{n} \quad (1)$$

where $\mathbf{n}$ is the direction vector defined by the tessellation.

Duits et al. [4] proposed a kernel implementation that solves the diffusion equation for HARDI images. We convolve this kernel with the ODF image, using the HARDI convolution in optimized C++, as described in [2]. We chose the parameters for the kernel in order to give a high relevance to the diffusion along the principal axis $D_{33} = 1.0, D_{44} = 0.003$ and $t = 5.0$, 4^{rd} order tessellation on the sphere and a $5 \times 5 \times 5$ neighbouring lattice. The convolution with such a kernel will result on the extrapolation of crossing profiles where the neighbourhood information so indicates, i.e., the E-ODFs.

C. Fiber population estimation

The fiber orientation estimation is based on the identification of the maxima on the estimated E-ODF profiles. In our implementation, maxima detection is performed using a numerical brute force algorithm applied on the discrete grid of the E-ODFs. Using region growing with a fixed threshold, multiple isolated regions from the spherical functions are segmented. In each of these regions, the local maximum is determined. The estimated fiber population is then exported back to Matlab.

Fig. 1. DTI versus E-ODFs for SNR=25. The E-ODFs are fit to real-valued spherical harmonic basis, and rendered on the GPU [5].

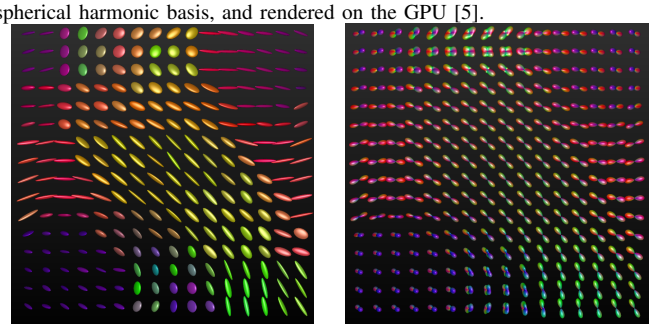

III. Results

Fig. 1 shows the estimated DTs, from a modest DTI acquisition scheme, and the extrapolated ODFs (slice z=5). Note the crossing profiles on middle-top and middle-bottom of the image.

IV. Conclusions

We show that modest acquisition schemes, with few gradient directions and low b-value=1000, can still deliver meaningful results. The contextual based processing method is able to extrapolate crossing information, while simultaneously smoothing out noise present in the images. As this is a contextual processing method, it is useless for the Isolated Voxels dataset. The diffusivity profile for each fiber is not accounted for in the current implementation, therefore we used the profile of a anisotropic tensor from the dataset. The brute-force maxima detection method is straightforward and easy to implement, but can be inaccurate if the subdivision order is chosen too low, or miss maxima if the threshold is too high. A ODF based fibertracking would provide a more clear view of the E-ODFs and the context. We believe that the notion of context would be much more explored in future, as it is a natural way of propagating diffusion on a space of positions and orientations, the native space of DWI.

References

[1] A. Barmpoutis et al., "A Unified Framework for Estimating Diffusion Tensors of any order with Symmetric Positive-Definite Constraints", ISBI (2010)
[2] P.R. Rodrigues et al., "Accelerated Diffusion Operators for Enhancing DW-MRI", VCBM (2010)
[3] V. Prckovska et al., "Extrapolating fiber crossings from DTI data. Can we gain similar information as HARDI?", CD-MRI, MICCAI (2010)
[4] R. Duits et al., "Left-invariant diffusions on the space of positions and orientations and their application to crossing-preserving smoothing of HARDI images." IJCV (2010)
[5] T.H.J.M. Peeters et al., "Fast and sleek glyph rendering for interactive HARDI data exploration". Visualization Symposium, IEEE Pacific (2009).

Parametric Dictionary Learning in Diffusion MRI

Sylvain Merlet*, Emmanuel Caruyer*, Aurobrata Ghosh* and Rachid Deriche*
* Athena Project-Team, Inria Sophia-Antipolis – Méditerranée

I. Introduction

In this work, we propose an approach to exploit the ability of compressive sensing to recover diffusion MRI signal and its characteristics from a limited number of samples. Our approach is threefold. First, we learn and design a parametric dictionary from a set of training diffusion data. This provides a highly sparse representation of the diffusion signal. The use of a parametric method presents several advantages: we design a continuous representation of the signal, from which we can analytically recover some features such as the ODF; besides, the dictionary we train is acquisition-independant. Next, we use this sparse representation to reconstruct the signal of interest, using cross-validation to assess the optimal regularization parameter for each signal reconstruction. The use of cross-validation is critical in the ℓ_1 minimization problem, as the choice of the parameter is sensitive to the noise level, the number of samples, and the data sparsity. Third, we use a polynomial approach to accurately extract ODF maxima. In the last section, we motivate and describe the choice of experimental parameters for the HARDI contest.

II. Parametric Dictionary Learning

A. Sparse reconstruction

We reconstruct the signal in an over-complete dictionary of continuous functions. Given a signal $\mathbf{y} \in \mathbb{R}^N$, this is expressed from the coefficient vector $\mathbf{x} \in \mathbb{R}^M$ as

$$\mathbf{y} = \mathbf{H}\mathbf{D}\mathbf{x} + \epsilon. \tag{1}$$

The matrix $\mathbf{H}$ is the standard $N \times R$ design matrix of the underlying family of continuous functions. The dictionary $\mathbf{D} \in \mathbb{R}^{R\times M}$, is a linear sparsifying transform, such that the signal $\mathbf{y}$ can be reconstructed from a limited number of atoms. This matrix does not depend on the choice of a specific acquisition protocol. The reconstruction is done by minimizing $||\mathbf{y} - \mathbf{H}\mathbf{D}\mathbf{x}||_2 + \lambda||\mathbf{x}||_1$. Here we propose to learn the dictionary $\mathbf{D}$ from a training dataset.

B. Parametric dictionary learning

We can rewrite Eq. 1 as $\mathbf{y} = \mathbf{H}\mathbf{c} + \epsilon$, and $\mathbf{c} = \mathbf{D}\mathbf{x}$. Given a training set of signals $\mathbf{Y}$ of size $N \times S$, we first estimate the coefficients $\mathbf{C} = (\mathbf{H}^{\mathrm{T}}\mathbf{H})^{-1}\mathbf{H}^{\mathrm{T}}\mathbf{Y}$. Then we look for a dictionary $\mathbf{D}$ of size $R \times M$ and a code $\mathbf{X}$ of size $M \times S$ verifying

$$\arg\min_{\mathbf{D},\mathbf{X}} ||\mathbf{C} - \mathbf{D}\mathbf{X}||_2^2 + \alpha||\mathbf{X}||_1, \text{ s.t. } \forall m \leq M, ||\mathbf{d}_m||_2 = 1 \tag{2}$$

with $\mathbf{d}_m$ the m^{th} column of $\mathbf{D}$. We use the python library scikit-learn [5] to solve this problem.

III. Cross-Validation

We use cross validation to assess λ [6]. In particular, we use a K-fold Cross Validation, which consists in splitting the entire data set in K subsets. $K-1$ subsets are used to reconstruct the signal whereas the K^{th} subset enables a tight estimation of regularization parameter λ_K via the evaluation of a cross validation distance. This operation is repeated K times by considering another subset. Then, we keep an average value, $\lambda = \frac{1}{K}\sum_{i=1}^{K}\lambda_i$. To avoid a drastic increase of the computational effort, we split our data set in 5 partitions, i.e. $K = 5$. Our previous experiments showed that it is sufficient to obtain a close approximation of the optimal λ.

IV. A Polynomial Approach for Maxima Extraction

The HARDI contest is based on fiber orientation estimation via the extraction of ODF maxima. After computing the ODF, we extract its maxima using a polynomial approach that can analytically bracket and numerically refine with high precision *all* maxima, ensuring that none are missed [4]. First, leveraging the linear bijection between the spherical harmonic basis and the homogeneous polynomial basis of the same order and degree, we rewrite the ODF as a polynomial, $\mathrm{P}(\mathbf{x} = [x_1, x_2, x_3])$, with $\|\mathbf{x}\|_2 = 1$. Second we formulate the optimization problem for computing the ODF extrema:

$$\partial F/\partial x_1 = \partial F/\partial x_2 = \partial F/\partial x_3 = \|\mathbf{x}\|_2^2 - 1 = 0, \tag{3}$$

where using Lagrange multipliers $F(\mathbf{x}, \Lambda) = \mathrm{P}(\mathbf{x}) - \Lambda\left(\|\mathbf{x}\|_2^2 - 1\right)$. However, instead of optimizing, which is inherently a local approach dependent on initializations, we solve the polynomial system Eq. 3 using a polynomial system solver that can analytically bracket all roots – missing none and refine them numerically to high precision. Finally, we identify the maxima from the extrema using the Bordered Hessian, which is the generalization of the Hessian.

V. Experimental parameters

For the HARDI contest, we choose $\mathbf{H}$ to be constituted of the continuous SPF basis functions [1], [2] and constrain our dictionary $\mathbf{D}$ to represent a combination of the SPF functions. We choose the SPF basis because it facilitates the ODF estimation [3]. We learn our dictionary on the training data set given for the HARDI contest. Then we probe the testing data set on 15 measurements uniformly spread on a single shell at b value $b = 2000\text{s} \cdot \text{mm}^{-2}$.

References

[1] H.E. Assemlal, D. Tschumperlé, and L. Brun. Efficient and robust computation of pdf features from diffusion mr signal. *Medical Image Analysis*, 13(5):715–729, 2009.

[2] Emmanuel Caruyer and Rachid Deriche. Optimal Regularization for MR Diffusion Signal Reconstruction. In *ISBI - 9th IEEE International Symposium on Biomedical Imaging*, Barcelona, Spain, May 2012.

[3] J. Cheng, A. Ghosh, R. Deriche, and T. Jiang. Model-free, regularized, fast, and robust analytical orientation distribution function estimation. In *MICCAI*, volume 6361 of *Lecture Notes in Computer Science*, pages 648–656. Springer, 2010.

[4] A. Ghosh, D. Wassermann, and R. Deriche. A polynomial approach for maxima extraction and its application to tractography in hardi. In Gábor Székely and Horst K. Hahn, editor, *IPMI*, volume 6801 of *Lecture Notes in Computer Science*, pages 723–734. Springer, jul 2011.

[5] F. Pedregosa, G. Varoquaux, A. Gramfort, V. Michel, B. Thirion, O. Grisel, M. Blondel, P. Prettenhofer, R. Weiss, V. Dubourg, J. Vanderplas, A. Passos, D. Cournapeau, M. Brucher, M. Perrot, and Duchesnay E. Scikit-learn: Machine learning in python. *Journal of Machine Learning Research*, 12:2825–2830, 2011.

[6] R. Ward. Compressed sensing with cross validation. *Information Theory, IEEE Transactions on*, 55(12):5773 –5782, 2009.

Sparse ℓ_1-ℓ_1 Multi-Tensor Imaging at the Price of DTI

Michael Paquette*, Maxime Descoteaux*
* Sherbrooke Connectivity Imaging Lab (SCIL), Computer Science department, Université de Sherbrooke

I. Introduction

Why use diffusion datasets to reconstruct the whole ODF if all we really need for some applications (ex. tractography) are the orientation of a few diffusion peaks? This question is even more important if we are limited to clinical applications for which only there is only time to acquire a diffusion tensor imaging (DTI)-like dataset (with 6 to 32 diffusion measurements). A more intuitive approach to make the best of the little data we have would be to fit a few one-peak model at each voxel. The diffusion tensor can be used as one such model [1]. In our technique, we then use a ℓ_1 data fitting term with a ℓ_1 sparsity regularization to fit the model to the signal. This ℓ_1-ℓ_1 is new in local diffusion estimation and allows us to use a general purpose linear program solver as opposed to the more common ℓ_2-ℓ_1 approach [3], [4].

II. Sparse Multi-Tensor Imaging

A. Problem statement

We want to approximate the diffusion signal S at q-points g_k with a sum of tensor T_i,

$$S_k = S_0 \sum_{i=1}^{M} f_i e^{-b g_k^t T_i g_k} + \epsilon,$$

where S_0 is the signal without diffusion weighting, f_i is the relative volume fraction of tensor T_i, M is the number of compartment, b is the diffusion sensitization strength and ϵ is the noise. We re-write our signal approximation as $S/S_0 = Uf + \epsilon$, where U is our dictionnary. We then search for a sparse and non-negative f^* so that Uf^* fits as best as possible the measured signal S. To do so, we solve the ℓ_1-ℓ_1 problem

$$f^* = \underset{f \geq 0}{\arg\min} \left[\|Uf - S\|_1 + \gamma \|f\|_1 \right],$$

where γ is the sparsity regularization constant used to adjust the trade-off between sparsity and data fitting.

B. Building the dictionnary

We build the dictionnary U from q-points g_i for $i = 1, 2, .., N$ uniformly spaced on one q-space shell (for one b-value), points p_j for $j = 1, 2, .., D$ evenly spaced on a half-sphere and tensor T. The j^{th} column of the dictionnary is the value of the diffusion defined by tensor T rotated at directions p_j at the q-points g_i i.e. $U_{ij} = e^{-b g_i^t T_j g_i}$, where T_j is T aligned to p_j.

C. Optimization

To solve the ℓ_1-ℓ_1 problem we re-casted it as a linear program [2] and used MATLAB's *LINPROG*. We used a fixed γ for the first pass and re-launched the optimization with different γ until f^* satisfied a norm concentration criterion

$$\frac{\|f_\alpha^*\|_1}{\|f^*\|_1} \geq \beta,$$

where $f_\alpha^* = Thresh_\alpha(f^*)$ (coefficients smaller than α are set to zero) and β is the minimum proportion of f^* ℓ_1-norm concentrated in it's few big coefficients i.e. the coefficients of f_α^*. Once f^* is determined, we first threshold it to remove the unwanted small components $f_\alpha^* = Thresh_\alpha(f^*)$. We then look at each maxima 2 by 2 and eliminate those with an angular distance smaller than δ as they are most likely representing the same diffusion peak. Sometimes the resulting vector $f_{\alpha,\delta}^*$ still has more peaks than a fixed μ, if so we remove the smallest intensity peak until we reach μ.

III. ISBI Hardi Contest

To fit the specific parameters of the contest, the maximum number of compartment μ was set to 3 and the tensor T used to build the dictionnary had eigenvalues $[\lambda_1\ \lambda_2\ \lambda_3] = [1.7\ 0.3\ 0.3] \times 10^{-3}$. The other parameters were tuned independently for each signal-to-noise ratio (SNR) (10, 20, 30) to first maximize the number of voxels where the right number of compartment was found and then to minimize the angular error. On the training data, we varied simulations with $N = 12, .., 50$ and b-values $= 500, .., 1500$. We found no significant amelioration of peak detection with high b-values while the angular error was affected by the SNR drop at higher b-values. The optimal trade-off between correct number of peaks and angle accuracy was obtained for low b-value and a low number of diffusion measurements. Therefore, the dataset asked for the ISBI contest was similar to a standard DTI with $N = 24$ diffusion measurements and $b = 750$ s/mm^2.

The final parameters were carefully set as $D = 500$ (dictionnary of size 500 tensors), initial $\gamma = 5$, $\beta = 0.5$, $\delta = 28.65^\circ$ and $[\alpha_{10}\ \alpha_{20}\ \alpha_{30}] = [0.15\ 0.13\ 0.11]$. These parameters, especially D, δ and α have a huge impact on the quality of the reconstruction as they define the maximum angular resolution of the method while controling the over-fitting (big noise peak where a tensor is fitted) and the under-fitting (true small peak discarted as noise). To estimate the volume fraction, we used the values of $f_{\alpha,\delta}^*$ normalized to sum to one. Since we also needed an ODF estimation for the contest, we further refined our estimation by trying different combinations of $[\lambda_1\ \lambda_2\ \lambda_3]$ in the contest's range $\left(\lambda_1 \in [1, 2] \times 10^{-3}, \lambda_2 = \lambda_3 \in [0.1, 0.6] \times 10^{-3}, FA \in [0.75, 0.9]\right)$ for each direction of $f_{\alpha,\delta}^*$ and chose the ones that minimized the residual with respect to the measured signal. We then used the analytical tensor ODF formula provided by the contest.

References

[1] Landman, B. a, Bogovic, J. a, Wan, H., Elshahaby, F. E. Z., Bazin, P.-L., and Prince, J. L. "Resolution of crossing fibers with constrained compressed sensing using diffusion tensor MRI". NeuroImage, 59(3), 2175-2186, 2012.

[2] Fu, H., k, Ng, M., Nikolova, M., l, Barlow, J., "Efficient Minimization Methods of Mixed l2-l1 and l1-l1 Norms for Image Restoration". SIAM J. Scientific Computing, 27(6), 1881-1902, 2006.

[3] Menzel, M. I., Tan, E. T., Khare, K., Sperl, J. I., King, K. F., Tao, X., Hardy, C. J., and Marinelli, L. "Accelerated diffusion spectrum imaging in the human brain using compressed sensing". Magnetic Resonance in Medicine, 66(5), 1226-33, 2011.

[4] Merlet, S., and Deriche, R. (2010). "Compressed Sensing for Accelerated EAP Recovery in Diffusion MRI". Computational diffusion MRI workshop, MICCAI (pp. 14-25). Beijing, China.

Diffusion Basis Functions on Spatially Regularized DW-MRI

Alonso Ramirez-Manzanares*, Ramon Aranda†, Mariano Rivera† and Omar Ocegueda†
* Department of Mathematics, University of Guanajuato
† Computer Science Department, Centro de Investigación en Matemáticas (CIMAT), A.C

I. Introduction

In the last years several methods have been developed in order to recover the axonal intra-voxel diffusion information on brain white mater from Diffusion Weighted Magnetic Resonance Images (DW-MRI). Some of them use a reconstruction based on a diffusion dictionary and the best as possible atom selection method to explain the DW-MRI signal into a voxel [1], [3]. In particular our group have developed state-of-the-art methods based on previous strategy, which also introduce intra and inter voxel regularization of the diffusion profiles [1], [4]. To propose a reconstruction solution in the "Hardi Reconstruction Contest Workshop 2012", we use some strategies we investigate in the past in order to present the best solution as possible as it is explained in the next section.

II. Methods

Here we explain the methodology we use in this contest.

A. Preprocessing Spatial regularization

In the case of the second phantom with spatial coherence ("Testing_SF") we apply a denoising step on the DW-MRI signals as we explain in the following. It is well known that the DW-MRI signal averaging over similar white matter voxels attenuates the acquisition noise and improves intra–voxel information estimation. However, signal averaging is a complicated task: due to the low spatial resolution on the DW images the averaging process can introduce dissimilar information to the voxel and corrupts the actual information. In this work we use two criteria in order to detect voxels sharing similar diffusion information. As in previous works [4], we use the information provided by the Diffusion Tensor Images (DTI) because this model (still lacking of intra–voxel information) it is quite robust to the noise effects for HARDI acquisition protocols. Given a voxel at a 3D position $r = [x, y, x]$ we take into account the set of 26 voxels belonging to its second-order 3D neighborhood $\mathcal{N}_r$. We analyze the difference between the Fractional Anisotropy coefficient (FA) and also, in order to introduce orientational information (axon bundle orientation), we select from the neighborhood only the voxels sharing a similar diffusion orientation. Based on previous strategy, we filter the DW-MRI using an adapting spatial averange:

$$\hat{S}_r = \frac{1}{n} \sum_{t:t\in\mathcal{N}_r^{SIM}} S_t \qquad (1)$$

where $\mathcal{N}_r^{SIM} \subseteq \mathcal{N}_r$ is the subset of neighboring voxels such that $|FA_r - FA_t| < TH_{FA}$ and also the angle between the main eigen–vector (principal diffusion direction) at r and the 1st or the 2nd eigen–vector at t is smaller than θ.

This work is supported by CONACYT México by SNI scholarships and student scholarships.

B. The DBF Method

In order to estimate intra voxel diffusion information we avoid the complex non-linear optimization problem associated to the fitting of the of Gaussians Mixture Model (GMM). For this reason, our group proposed a strategy for recovering multi-DTs at axonal fiber crossing regions [1]. We relaxed the problem by using a fixed set of Diffusion Basis Functions (DBF) $\Phi = [\phi_{1,1}, \phi_{2,1}, ..., \phi_{L,P}]$ (where L is the total number of applied gradients and P is the total number of base tensors). This set is not complete because is a discretization on a orientational 3D space. In this model, $\phi_{i,p}$ is the diffusion weighted signal associated to the gradient vector g_i and a fixed tensor base $\bar{T}_p$. By using this model it is possible to solve the GMM by means of a linear equation system with constrains. A limitation of this approach is that the diffusion profile is not estimated: the method reports an average diffusion profile for all the recovered multi-tensors. To transform the solution from the discrete space (the DBF dictionary) to the continuos 3D orientational space we use the clustering heuristic reported on [1].

III. Implementation Details and Parameters

We use an acquisition protocol composed of 48 diffusion encoding orientations with an homogeneous $b = 1500$ value.

For the spatial signal regularization we use the following values $TH_{FA} = 0.1$. We observe it is convenient to set the θ value according the amount of signal noise, we set $\theta_{SNR=5}$ = $\theta_{SNR=10}$ = 15^o, $\theta_{SNR=15}$ = $\theta_{SNR=20}$ = 12^o, $\theta_{SNR=25}$ = $\theta_{SNR=30}$ = 10^o, and $\theta_{SNR=35}$ = $\theta_{SNR=40}$ = 8.

For the DBF method we use a diffusion dictionary with 129 diffusion directions uniformly distributed over the half–sphere. Based on previous studies [2] and experiments on the training data, we know that the DBF method is prone to over estimate the number of diffusion compartments. In order to overcome the overestimation behavior we eliminate Multi-DTs with a size compartment smaller than 30% of the biggest size compartment within a voxel. In the discrete–to–continuos–orientation DBF step, we set a 16-size neighborhood on the basis directions for the spatially coherent phantom, on the other hand, on the 'Testing_IV" phantom, composed of non spatially related voxels, we set a 6-size neighborhood on the basis directions.

References

[1] A. Ramirez-Manzanares , M. Rivera, B. C. Vemuri, P. Carney and T. Mareci, "Diffusion basis functions decomposition for estimating white matter intravoxel fiber geometry", IEEE Trans. Med. Imaging., 26(8), 1091–1102 (2007).
[2] A. Ramirez-Manzanares, P. A. Cook, M. Hall, M. Ashtari and J. C. Gee, "Resolving Axon Fiber Crossings at Clinical b-values: An Evaluation Study", Journal of Medical Physics, 38(9), 5239-53 (2011).
[3] B. Jian, B. C. Vemuri, "A unified computational framework for deconvolution to reconstruct multiple fibers from DW-MRI", IEEE Trans. Med. Imaging., 26(11), 1464–1471, (2007).
[4] A. Ramirez-Manzanares, H. Zhang, M. Rivera, and J. C. Gee, "Robust regularization for the estimation of intra-voxel axon fiber orientations", In Workshop Math Methods in Biomed Imag Anal, Anchorage, Alaska, 1-8, (2008).

Compressed Sensing Reconstruction of Multi-Tensor Models

Merry Mani*, Mathews Jacob† and Jianhui Zhong*
* University of Rochester, NY,USA,† University of Iowa, IA, USA

I. Introduction

With single tensor model being inadequate to represent the heterogeneous diffusion pattern in the imaged voxels of a diffusion weighted image, several variants of the model, especially multi-tensor model, was studied to explore their utility in modeling the same. Multi-tensor model assumes the diffusion in each voxel as a linear combination of diffusion in various directions, each of which can be independently represented using a single tensor. The challenges the multi-tensor model had to face was the following: (i) the number of tensors in each voxel was not known a-priori, (ii) the unknown tensor elements was hard to solve due to the non-linear nature, when more than one tensor was present, (iii) with increasing unknowns, more diffusion direction measurements were required, (iv) complex algorithms with multiple restarts were required to solve the multi-tensor model, all of which rendered it an unattractive model. In [1], Ramirez-Manzanares et al rejuvenated the above model with a new framework using a discrete set of diffusion basis functions that spanned the q-space uniformly. By parameterizing diffusion along these basis functions, they were able to reconstruct the multiple fiber orientations accurately. Our interest in the above method is motivated by the application of the framework to solve the problem of accelerating high spatial and angular resolution diffusion imaging. Exploring a solution to the above problem revealed some weaknesses in the current diffusion modeling schemes, which we discuss later. We however, first describe the algorithm that was used to solve the challenge datasets, which is not conceptually different from [1][2].

II. Method

We express the real part of the diffusion weighted signal as a linear combination of a number of diffusion basis functions,

$$S(b,\mathbf{g}) = S_0 * \sum_{i=1}^{N} f_i \ .\psi_i(b,\mathbf{g}). \tag{1}$$

The basis functions are formed by a set of oriented Gaussians, $\psi_i(b,\mathbf{g}) = e^{-b\mathbf{g}^T\mathbf{D}_i\mathbf{g}}$. These basis functions are generated by rotating a base tensor $\mathbf{D} = 1e^{-3} * [300\ 0\ 0; 0\ 300\ 0; 0\ 0\ 1700]$ along a set of basis directions to obtain $\mathbf{D}_i = \mathbf{R}_i * \mathbf{D} * \mathbf{R}_i{}^T; i = 1:N$. N=256 basis directions that uniformly span the q-space are considered and the basis functions ψ_i corresponding to the N directions are precomputed. With K diffusion measurements using diffusion gradient $\mathbf{g}_k$, $K < N$, we get K linear equations of the form (1). The unknowns in the set of equations are the N coefficients of the Gaussians. These set of equations can be written in matrix form as $\mathbf{y} = \mathbf{\Psi f} + \epsilon$, where $\mathbf{\Psi}_{i,j} = \psi_j(b,\mathbf{g}_i)$, $\mathbf{y}$ and $\mathbf{f}$ are the vectors comprising of the measured signal and unknowns respectively. ϵ is the noise that is Rician distributed. A few assumptions can be used to aid the recovery of the unknown vector $\mathbf{f}$: (i) it is reasonable to assume that, in a voxel comprising to white matter tissue alone, the number of possible diffusion directions will be sparse, (ii) the white matter bundles are also spatially connected, thus exhibiting a structure. Using these two assumptions, we can come up with a non-linear optimization scheme to solve for $\mathbf{f}$ as follows:

$$\begin{aligned} \hat{\mathbf{f}} &= \underset{f}{\operatorname{argmin}} ||\mathbf{\Psi f} - \mathbf{y}||_{l2}^2 + \lambda_1||\mathbf{f}||_{l1} + \lambda_2||\mathbf{f}||_{l_{TV}} \\ &\text{where } ||\mathbf{f}||_{l1} = \sum_i |\mathbf{f}_i| \text{ and } ||\mathbf{f}||_{l_{TV}} = ||\nabla\mathbf{f}||_{l1} \end{aligned} \tag{2}$$

The first term in the cost function enforces data consistency, the second term enforces sparsity on the coefficients of the basis functions and the third term enforces spatial smoothness on the coefficients by using a total-variation regularization. By re-writing the ℓ_1 norm as an iterative re-weighted ℓ_2 norm, the above cost function is solved using a conjugate gradient algorithm. In the case where it is known a-priori that there is no spatial dependence between voxels (as in the case of the isolated voxel dataset), λ_1 is set to zero. In all other cases, the value of λ_1 and λ_2 needs to be determined. In the particular case of the challenge dataset, this could be easily done by optimizing the λs on the training dataset by picking the λ that gives the minimum reconstruction error, and using these values on the testing dataset. The conjugate gradient steps and the iterative re-weighting are applied until the cost function converges to the minimum. The ODF can then be computed using the recovered $\mathbf{f}$. In our results, we have used K= 30 directions and a b-value of $1200s/mm^2$.

III. Discussion

The diffusion basis functions framework provides a convenient formulation to detect the orientational heterogeneity in the white matter voxels and is ideal for a compressed sensing reconstruction enabling the recovery of high angular resolution information from a few diffusion measurements. Although, a base tensor needs to be assumed with fixed diffusivity values, the above approximation works well for a range of diffusivity values, with no significant performance degradation with small deviations of diffusivities. However, in practical situations, a given voxel will likely have gray matter and white matter tissues. An appropriate model for such case will be a partial volume model, where there is a component to represent isotropic diffusion as well. Another aspect that is overlooked in these schemes is that the reconstructions are not adapted for Rician noise distributions. The commonly considered quadratic cost function formulation becomes equivalent to the maximum likelihood estimation if the noise model were Gaussian. Since this is not true when considering only the real part of the diffusion signal, we propose reconstruction directly from complex k-space data where noise is Gaussian. This in turn calls for a complex diffusion signal model. An added advantage of reconstructing from k-space data is the flexibility in designing the k-space trajectories to suit special needs. In the case of our application for accelerating high spatial and angular resolution diffusion imaging, we concluded that by under-sampling the combined k-q domain, we could achieve a higher acceleration than under-sampling in the q-domain alone. We used a complex diffusion model based on the partial volume model and jointly reconstructed the coefficients in all voxels from complex under-sampled k-q space data. Please see [3] for details.

REFERENCES

[1] A. Ramirez-Manzanares, M. Rivera, B. C Vemuri, P. Carney, and T. Mareci, "Diffusion basis functions decomposition for estimating white matter intravoxel fiber geometry." *IEEE Transactions on Medical Imaging*, vol. 26, no. 8, pp. 1091–1102, 2007.

[2] B. A. Landman, H. Wan, J. A. Bogovic, P.-L. Bazin, and J. L. Prince, "Resolution of Crossing Fibers with Constrained Compressed Sensing using Traditional Diffusion Tensor MRI." *Proceedings - Society of Photo-Optical Instrumentation Engineers*, vol. 7623, no. 8, p. 76231H, Jan. 2010.

[3] Mani M,Jacob M, Guidon A , Liu C , Song A, Magnotta V and Zhong J, "Acceleration of High Angular and Spatial Resolution Diffusion Imaging Using Compressed Sensing," *ISBI*, 2012.

L1-based ODF Estimation with Total Generalized Variation

M. Reisert, H. Skibbe and V.G. Kiselev
Medical Physics, University Medical Center Freiburg, Freiburg, Baden Württemberg, Germany,

UNIVERSITY FREIBURG HOSPITAL

Introduction: There are a variety of methods for the estimation of the ensemble averaged diffusion propagator (EAP) and the derived orientation distribution function (ODF) [3,4,5]. Our method uses basically three ideas to get a reliable estimate: 1) there is a sparse representation of the EAP in terms of carefully selected basis functions. 2) the EAP is positive. 3) The EAP is spatially coherent. Similar ideas were also used in [5], that is, sparsity together with a spatial prior based on Total Variation. In literature one can find various proposal for different kind of basis functions. As the signal in spherical harmonic respresentation is not sparse, we decided for a simple sum of exponentials (left), where N is the number of discrete directions on the sphere and M the number of different parameter sets of fixed decay-rates. The goal is to find the coefficient fields $c_{k,i}(\mathbf{r})$ such that the predicted signal S explains the measurement. All other parameters are fixed. The sparsity assumption can be realized by a L1-norm regularization of the coefficient fields. As spatial prior we use a generalization of the Total Variation (TV) regularizer. While the usual TV-prior tends to produce so-called staircasing artefacts, the Total Generalized Variation (TGV) [2] controls this effect much better. We use TGV of order 2, which prefers spatially linear trends (instead of a constant like TV). Our final cost-function looks like (left). For optimization we use a primal-dual approach of Chambolle & Pock [1], which is able to deal with all our demands: L1-based regularizers and the positivity constraint on the coefficient fields. Once the coefficient fields are determined anything can be computed from our analytical signal model. Based on the Fourier transform of the model we reconstructed the ODF on the 724-point sphere and determined the local maxima of the ODF as fiber compartements.

$$S(\mathbf{r},\mathbf{q}) = \sum_{k=1}^{N}\sum_{i=1}^{M} c_{k,i}(\mathbf{r})\; e^{-D_i^{\mathrm{fib}}(\mathbf{n}_k^T\mathbf{q})^2 - D_i^{\mathrm{iso}}q^2}$$

$$J(c) = \frac{1}{\sigma^2}||S(c) - S_{\mathrm{meas}}||_2^2 + \lambda_1||c||_1 + \lambda_2 \mathrm{TGV}^2(c)$$

Parmeter And Gradient Selection: The important parameters of our model are the shape of the basis functions in terms of decay-rates and the strengths of the regularizing terms. The parameters were determined partially be visual inspection and grid searching. We decided for a q-space distribution such that the spatial regularizer can help significantly to improve the estimate. For example for a full sampling with 257 points it was quite hard to find a setting such that TGV can improve the results even for a SNR of 10. So, we used 32 directions on a 1500 b-shell and the same 32 directions on a 2500 b-shell, i.e. overall 64 measurements.

Results: As an example we show in Figure 1 visual results for the diffusion ODF with SNR=10,30 with and without spatial regularization on the 2D phantom provided. For all cases the same regularization strength are used. We also evaluated the proposed quality measures: difference of fiber compartments (DC), angular precision (AP) and the mean error of the ODF (ME). Figure 2 shows the corresponding numbers for the IV phantom and the 3DSF phantom where all parameters are set as given below.

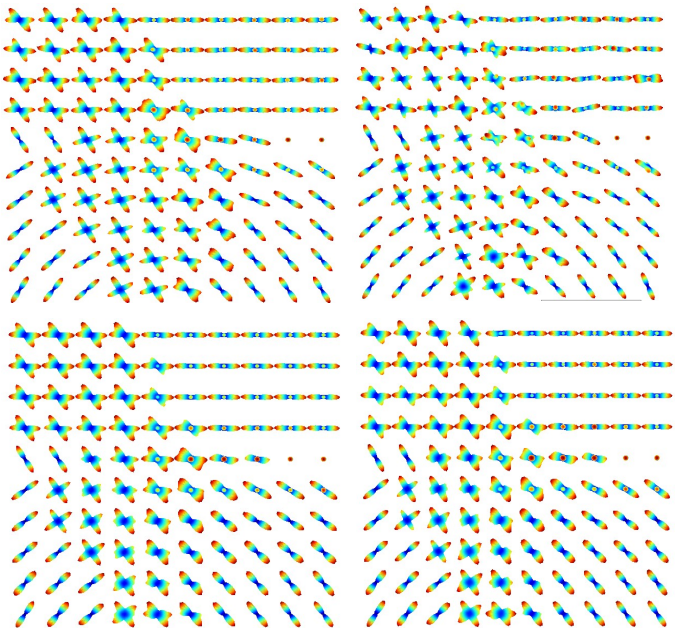

Figure 1: Top: ODF for SNR=30 (left) and SNR=10 (right) without spatial regularization. Bottom: ODF for SNR=30 (left) and SNR=10 (right) with TGV-spatial regularization.

SNR/phantom	10/SF	20/SF	30/SF	10/IV	20/IV	30/IV
DC (%)	2.5	2.5	2.5	22.8	22.6	21.9
ME (%)	1.2	0.4	0.3	4.7	2.1	1.3
AP (°)	3	2.1	2	9.3	5.8	4.8

Figure 2: Performance measures on two training data sets (SF is the 3D phantom). SF with TGV-regularization, IV without TGV-regularization for a SNR=10,20,30. The measures (DC) and (ME) are given in percent, (AP) in degree.

Competetion Setting: We used M=2 types of different decay rates, namely D^{fib} = [0.85 , 1.65] and D^{iso} = [0.15 , 0.25] and N=256 direction equidistributed on the sphere, i.e. overall 512 basis functions. The cost-parameters for the SF-case were set to $\sigma = 1/\mathrm{SNR}$ and correspondingly for SNR=[10,20,30] we have set λ_1= [10 , 20, 45] and λ_2= [2 , 4, 4]. For the IV-case we have set λ_1= [20 , 20, 30].

References: *[1] Antonin Chambolle, Thomas Pock: A First-Order Primal-Dual Algorithm for Convex Problems with Applications to Imaging. Journal of Mathematical Imaging and Vision 40(1): 120-145 (2011) [2] Kristian Bredies, Karl Kunisch and Thomas Pock. Total generalized variation. SIAM Journal on Imaging Sciences, 3(3):492-526, 2010. [3] Tuch. Q-ball imaging. Magnetic Resonance in Medicine, 52: 1358–1372 (2004) [4] Canales-Rodriguez et al. Mathematical description of q-space in spherical coordinates: exact q-ball imaging. Magnetic Resonance in Medicine, 61: 1350–1367 (2009) [5] Michailovic et al. Spatially regularized compressed sensing for high angular resolution diffusion imaging. IEEE TMI, 30: 1100-1115 (2011)*

Diffusion Tensor Reconstruction Using Periodic Spiral Imaging

Farshid Sepehrband, Jeiran Choupan, Viktor Vegh, Quang Tieng, David Reutens and Zhengyi Yang*
Centre for Advanced Imaging
The University of Queensland
Brisbane, Australia
{f.sepehrband, j.choupan}@uq.edu.au; {viktor.vegh, quang.tieng, david.reutens, zhengyi.yang}@cai.uq.edu.au

Abstract— **A new q-space sampling scheme is proposed to identify single and multiple fibre orientations within voxels derived from diffusion-weighted images. Diffusion data were obtained by defining a spiral trajectory of gradient direction samples. The number of gradient directions used to generate raw data corresponds to the spiral trajectory discretization. We used a fixed angle between adjacent gradient directions. This led to information with inherent periodicity of the diffusion signal. We exploited the trends in the signal to first denoise the data and then to identify fibre orientations. We applied our method to synthetic data (SNR=10, 20 and 30) and identified single and multiple fibres within voxels with a mean error of 9 degrees.**

Keywords- spiral sampling; periodocity; denoising; diffusion-weighted imaging.

I. INTRODUCTION

Diffusion Weighted Imaging (DWI) quantifies molecular motion as a consequence of diffusion [1]. Eigen-values and corresponding vectors in Diffusion Tensor Imaging (DTI) have been used to obtain white matter connectivity maps of neural networks [2]. Specific approaches, namely Q-ball, DSI, CHARMED, GQI and CSD [3-7], have been proposed to resolve multiple diffusion directions. These methods require a large number of gradient directions, increasing imaging time and impacting clinical utility, and high b-values. Moreover, because of noisy data, it has been difficult to resolve multiple fibres with orientation differences of less than 30 degrees. We propose a new approach to resolving these issues based on spiral sampling of q-space.

II. METHOD

A. Outline

The following steps are involved in the tensor reconstruction: (a) specify sampling scheme, (b) acquire DWI data, (c) denoise periodic DWI data using Fourier filtering, (d) explore periodic patterns in filtered data, (e) identify locations of signal attenuation corresponding to fibre orientation, (f) calculate fibre orientations, and (g) compute diffusion tensor given the fibre orientation. To obtain the diffusion tensor for each fibre orientation, we reformulated the eigen decomposition of the generalized tensor equation and incorporated the principal direction identified in (f). The novelty of our method lies in the sampling scheme employed, because it allows filtering of periodic data and the extraction of fibre orientation based on periodic signal attenuation.

B. Sampling Scheme

A q-space spiral sampling scheme over a sphere using constant angular steps was employed (Fig. 1). The sampling trajectory was defined in Cartesian coordinates as:

$$x = \sin(rt/2\pi)\cos(t), \quad y = \sin(rt/2\pi)\sin(t), \quad z = \cos(rt/2\pi), \qquad (1)$$

where r and t are angular steps in the azimuth and zenith coordinate directions. Consecutive arrangement of the DWI data enabled investigation of the periodicity of the diffusion signal.

C. Denoising of DWI data

Denoising was performed by first taking the Fourier transform (FT) of the DWI data arranged in accordance with the sampling scheme. A low-pass filter was then applied, retaining one half of the original signal. The denoised signal was reconstructed by computing the inverse FT of the low-pass filtered data. An example is provided in Fig. 1.

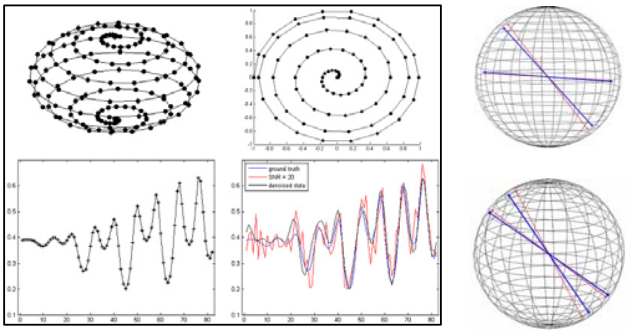

Fig. 1. Left panel: Spiral sampling scheme (Top row); the periodic DWI signal without noise and noisy signal (SNR=20) compared with denoising result (Bottom row). Right panel: examples of the actual (red) and estimated (blue) orientations of the crossing fibres in two voxels.

III. SIMULATION RESULT

For the synthetic data, 82 gradient directions and a b-value of 1200s/mm^2 were used. On the right panel of Fig. 1 two examples of multiple fibre orientations within an image voxel for the case when SNR = 20 is provided. The top figure shows the actual fibre orientations (red) and computed orientations (blue). The angle between the actual fibres was 44 degrees. The deviation between the actual and computed orientations was less than 5 degrees. Similarly, the bottom right figure illustrates the case when the angle between fibres was 24 degrees. In this case, orientation could be calculated to within 6 degrees accuracy. On average, we resolved fibre orientations with a mean error of 9 degrees. In conclusion, we were able to exploit signal periodicity for signal denoising, and local minima of the periodic DWI data were used to define fibre orientations.

REFERENCES

[1] P. J. Basser, *et al.*, "MR diffusion tensor spectroscopy and imaging," *Biophysical journal*, vol. 66, pp. 259-267, 1994.

[2] S. Mori and P. B. Barker, "Diffusion magnetic resonance imaging: its principle and applications," Anat Rec, vol. 257, pp. 102-109, 1999.

[3] D. S. Tuch, "Q-ball imaging," Magnetic resonance in medicine, vol. 52, pp. 1358-1372, 2004.

[4] V. J. Wedeen, et al., "Diffusion spectrum magnetic resonance imaging (DSI) tractography of crossing fibers," NeuroImage, vol. 41, pp. 1267-1277, 2008.

[5] Y. Fang-Cheng, et al., "Generalized q-Sampling Imaging," Medical Imaging, IEEE Transactions on, vol. 29, pp. 1626-1635, 2010.

[6] Y. Assaf and P. J. Basser, "Composite hindered and restricted model of diffusion (CHARMED) MR imaging of the human brain," Neuroimage, vol. 27, pp. 48-58, 2005.

[7] J. D. Tournier, et al., "Direct estimation of the fiber orientation density function from diffusion-weighted MRI data using spherical deconvolution," NeuroImage, vol. 23, pp. 1176-1185, 2004.